Growth patterns of caudal fin rays are informed by both external signals from the regenerating organ and remembered identity autonomous to the local tissue

Melody Autumn[1], Yinan Hu[1], Jenny Zeng[1], and Sarah K. McMenamin[1‡]

[1]Biology Department, Boston College, Chestnut Hill, MA 02467
[‡]Author for correspondence: mcmenams@bc.edu, Higgins Hall 360, 140 Commonwealth Avenue, Chestnut Hill, MA 02467

Author contributions: M.A., Y.H., and S.K.M. designed research; M.A., Y.H., and J.Z. performed research; M.A., Y.H., and S.K.M. analyzed data; and M.A. and S.K.M. wrote the paper.

HIGHLIGHTS

- Gene expression patterns during fin regeneration correspond with proximodistal location.
- Distal portions of rays transplanted to proximal regions retain positional identity that can influence their growth rate and length during regeneration.
- Location of ray bifurcations and length of segments along the proximodistal axis are determined by the regenerative environment.

ABSTRACT

Regenerating tissues must remember or interpret their spatial position, using this information to restore original size and patterning. The external skeleton of the zebrafish caudal fin is composed of 18 rays; after any portion of the fin is amputated, position-dependent regenerative growth restores each ray to its original length. We tested for transcriptional differences during regeneration of proximal versus distal tissues and identified 489 genes that differed in proximodistal expression. Thyroid hormone directs multiple aspects of ray patterning along the proximodistal axis, and we identified 364 transcripts showing a proximodistal expression pattern that was dependent on thyroid hormone context. To test what aspects of ray positional identity are directed by extrinsic cues versus remembered identity autonomous to the tissue itself, we transplanted distal portions of rays to proximal environments and evaluated regeneration within the new location. While neighboring proximal tissue showed robust expression of *scpp7*, a transcript with thyroid-regulated proximal enrichment, regenerating rays originating from transplanted distal tissue showed reduced (distal-like) expression during outgrowth. These distal-to-proximal transplants regenerated far beyond the length of the graft itself, indicating that cues from the proximal environment promoted additional growth. Nonetheless, these transplants initially regenerated at a much slower rate compared to controls, suggesting retained memory of distal identity. This early growth retardation caused rays that originated from transplants to become noticeably shorter than their native neighboring rays. While several aspects of fin ray morphology (bifurcation, segment length) were found to be determined by the environment, regeneration speed and ray length are remembered autonomously by tissues, persisting across multiple rounds of amputation and regeneration.

KEYWORDS

Regeneration, Zebrafish, Transplant, Growth rate, Skeletal patterning, Thyroid hormone

INTRODUCTION

To restore the original morphology of an appendage, regeneration must faithfully rebuild lost tissue. The morphology and size to which regenerating tissue grows must be determined by positional information (Wolpert, 1969). Such cues could be informed by remembered positional identity or could be interpreted from environmental cues from surrounding tissue (e.g. diffusible or spatially distributed factors). However, these two potential inputs can be difficult to disentangle.

Zebrafish fins are powerful models for studying regeneration and can provide new insights into the nature of positional memory and the pathways that regulate regional growth and patterning. The caudal fin is made up of symmetrical dorsal and ventral lobes, each composed of nine segmented fin rays. Upon amputation, a blastema of de-differentiated cells forms (Knopf et al., 2011; Tu & Johnson, 2011), and each ray regrows from the wound site to rebuild its original morphology (as reviewed in Harris et al., 2021; I. M. Sehring & Weidinger, 2020).

Regeneration rate is informed by the relative proximodistal location of the regenerating tissue on the fin (Lee et al., 2005). Distal amputations are followed by slow regenerative growth, while proximal amputations close to the body initiate rapid growth that progressively slows as the regenerate approaches the original size (Akimenko et al., 1995; Banu et al., 2022; Lee et al., 2005; Uemoto et al., 2020). Regardless of how much tissue is removed, regeneration restores the organ to its original size within three weeks (Wehner et al., 2014).

Intact fin rays exhibit morphological differences along the proximodistal axis. At the proximal base, ray segments are longest and widest, tapering and shortening progressively towards the distal edge; rays also form bifurcations at specific locations along the axis (Harper et al., 2023). Components of proximodistal patterning are regulated by thyroid hormone (TH), which induces distal features (Harper et al., 2023). Proximal and distal tissues from intact adult fins show unique transcriptomic profiles (Rabinowitz et al., 2017), and these expression patterns are regulated by TH (Harper et al., 2023). Here, we tested if transcriptomic differences are apparent during the regeneration of proximal tissues as compared to distal regions of the fin.

The relative length of individual rays appears to be remembered autonomously by tissues (Uemoto et al., 2020). Fin rays differ in length from the central to the peripheral regions of the fin, giving the organ an overall forked shape. Previous transplantation experiments demonstrate that when short central rays are swapped with long peripheral rays, the tissue regenerating in the new environment produces a ray of intermediate length (Shibata et al., 2018). However, it remains unclear whether proximodistal location along an intact ray imprints remembered positional information that could inform morphology during regeneration.

Transplants of blastema cells from different proximodistal locations were not able to influence lengths of regenerates (Shibata et al., 2018). Further, hemi-rays—the apposed contralateral bones that make up individual ray segments—can be transplanted to different proximodistal locations; the resulting recombinant rays regenerate with morphologies expected for the regenerating environment (Murciano et al., 2007). Nonetheless, given the notable differences in gene expression and morphology along the intact proximodistal axis, we asked if entire ray segments could remember proximodistal identity, testing the ability of this memory to influence gene expression, regrowth rates, ultimate length, and patterning of regenerating rays.

RESULTS

Regenerating fin tissue shows unique proximodistal transcription. We predicted that regenerating tissues would show unique expression patterns during the regrowth of different proximodistal regions. Amputating at a consistent proximal location, we evaluated expression from three regions as they regenerated: a proximal region collected after the blastema had

already formed (Wang et al., 2019; 4 days post amputation, dpa), a middle region midway through regeneration as the ray bifurcations were forming (7 dpa), and a distal region (15 dpa; see Supplementary Fig. 1C). We identified 489 genes that are differentially expressed between proximal and distal regenerating tissue (Fig. 1): 29 genes were proximally enriched and 460 were distally enriched. A GO term analysis of differentially expressed transcripts showed enrichment of genes involved in pigmentation and gas transport (Supplementary Fig. 1G). In our regenerates, ray bifurcations were forming during the middle time point (7 dpa); however, this tissue revealed no transcripts that were differentially expressed compared to proximal and distal tissues.

Thyroid hormone maintains the proximodistal expression of many genes. Developmental hypothyroidism proximalizes both transcriptional expression and ray morphology in intact fins (Harper et al., 2023), and we asked if fins regenerating in a hypothyroid context also showed proximalized gene expression patterns. Analyzing the transcriptomes holistically, the major axes of variation robustly captured proximodistal location (dimension 1) and TH condition (dimension 2), but there was little apparent correlation between the two (Fig. 1A). Nonetheless, certain transcripts showed a proximodistal differential in expression that was dependent on the presence of TH. Indeed, of the 489 differentially expressed genes found in WT tissue, 364 lost proximodistal specificity in hypothyroid tissue: ~86% (25/29) of proximally enriched and ~76% (349/460) of distally enriched genes lost proximodistal differential expression in a hypothyroid context.

***scpp7* is proximally enriched during regeneration.** Since distal-specific morphologies are regulated by TH (Harper et al., 2023), genes that are expressed in a TH-dependent proximodistal differential are strong candidates for involvement in distal patterning. Of the transcripts showing TH-dependent proximal enrichment, we selected secretory calcium-binding phosphoprotein 7 (*scpp7*). Along with other SCPP factors, SCPP7 is involved in bone mineralization (Kawasaki, 2009), and is strongly upregulated during scale regeneration (Bergen et al., 2022). Proximal tissues showed robust expression of *scpp7* in both WT and hypothyroid backgrounds, but the gene was more robustly expressed in distal tissue from hypothyroid regenerates compared to those of WT (Fig. 1C-H).

We asked if the variation in *scpp7* expression in the different regions could be attributed to differences in the time since injury rather than proximodistal position of regeneration. To test this possibility, we performed distal amputations on WT fins (Supplementary Fig. 1D) and assessed *scpp7* expression in 4 dpa distally-regenerating tissue. *scpp7* expression was similar to that of 15 dpa distally-regenerating tissues (Supplementary Fig. 1E-F), suggesting that this expression differential indeed characterizes distal tissue.

***scpp7* expression in regenerating tissues reflects original proximodistal location rather than regenerative environment.** We asked whether attenuated *scpp7* expression would be remembered by distal tissues if they regenerated in a proximal context. To test this, we designed a distal-to-proximal ray transplantation in which a ray was removed from the fin, and a distal portion of the extirpated ray is transplanted into the proximal position. After the distal transplant integrates into the proximal location, the entire fin was amputated (including the transplant) to allow distal tissue to regenerate alongside proximal tissue (“dist-to-prox”, Fig. 2A-C). A completely extirpated ray with no transplant produced no regeneration (Supplementary Fig. 2). We assessed *scpp7* expression in the regenerate originating from the dist-to-prox transplant and found expression was significantly reduced compared to those of neighboring proximal rays at 4 dpa (Fig. 2D-E). This recapitulation of distal-like expression while regenerating in a proximal context suggests that expression level of this transcript is informed by autonomous tissue identity and is not merely the result of environmental cues.

Distal-to-proximal transplanted tissue restores shorter fin rays. We predicted that if dist-to-prox transplanted tissue possessed remembered positional identity, precocious distal features should be apparent in the resulting regenerate. To adequately evaluate subtle differences in regrowth, we needed a comparison that had undergone identical microsurgery without introducing any major positional translocation. Thus, we performed control “prox-to-prox" transplants, extirpating the ray, then grafting the entire tissue back into its position (Fig. 3A-D). Interestingly, these prox-to-prox rays were not able to regenerate to the same length as the corresponding rays on the ventral lobe (Supplementary Fig. 3K) and were ultimately slightly shorter than undisturbed neighboring rays. During microsurgery, prox-to-prox rays inevitably lost 1-3 segments (Supplementary Fig. 3I), so this slight positional shift and/or the microsurgery itself are sufficient to effect patterns of regeneration.

Even compared to the microsurgery-controlled baseline of prox-to-prox rays, rays originating from dist-to-prox transplants were consistently shorter, through eleven weeks after amputation (Fig. 3I). Dist-to-prox regenerates were obviously shorter than both neighboring rays (Fig. 3G-H) and the corresponding ray on the ventral lobe (Supplementary Fig. 3G-H). These differences in ultimate length suggest that the dist-to-prox rays indeed retain a memory of their original proximodistal identity.

Growth rates during regeneration reflect both intrinsic identity and environmental context. Since the dist-to-prox regenerates were significantly shorter compared to prox-to-prox regenerates, we asked whether these regenerates grew at a relatively slower pace. During the first week of regeneration (weeks 0-1), prox-to-prox transplants regenerated rapidly, adding 2.6 mm (0.37 mm per day); in contrast, dist-to-prox regenerates grew much more slowly, adding only 2.0 mm during this first week (0.27 mm per day; Fig. 3J-K). By the second week (weeks 1-2), the two types of transplants were growing at comparable speeds, adding 1.9 mm length (0.27 mm per day). Through the remainder of the eleven week period, dist-to-prox and prox-to-prox rays maintained similar regrowth speeds (Fig. 3J-K). Growth rates plateaued after week nine, as the regenerates reached isometric growth (Fig. 3J-K). Prox-to-prox rays’ regrowth speed was reduced in comparison to corresponding ventral rays during the first week of regeneration but by the second week they kept pace (Supplementary Fig. 3J-K).

Fin ray patterning is environmentally coordinated. Bifurcations are a discrete indicator of proximodistal morphology (Harper et al., 2023). We asked whether the origin of tissue (distal versus proximal) would influence the location of the bifurcation in a regenerate, and quantified the bifurcation position in dist-to-prox and prox-to-prox rays. Bifurcations formed in the location expected for the environment regardless of transplant type (Fig. 4C), suggesting bifurcation position is the result of globally coordinated cues rather than being locally regulated by tissues based on remembered identity.

While ray length is similar between dorsal and ventral lobes, we found that the proximodistal patterning differs (Supplementary Fig. 4). Regenerated ray segments were found to be somewhat longer and wider than segments of the intact fin (Supplementary Fig. 5E-F; Supplementary Fig. 6I-J). We asked if segment morphology reflected positional memory of the tissue or else was guided by environmental cues. While dist-to-prox rays regrew marginally thinner segments, segment length was comparable to that of prox-to-prox ray segments (Fig. 4D-E). Regenerating fin length can be pharmacologically increased without changing positional identity (Daane et al., 2018), and we found induced altered proximodistal patterning also goes unremembered in future regeneration cycles (Supplementary Fig. 8).

Rays originating from distal transplants remember their length through multiple rounds of regeneration. To test whether the intermediate length of dist-to-prox rays would be

remembered, we performed multiple rounds of regeneration, amputating distal to the previous amputation plane (Fig. 5A-D). Even after three rounds of regeneration, rays originating from dist-to-prox transplants were always significantly shorter than corresponding ventral rays (Fig. 5E-G).

DISCUSSION

Intact fins show transcriptomic differences across the proximodistal axis (Harper et al., 2023; Rabinowitz et al., 2017), and here we identified a robust suite of gene expression patterns that shift as the fin regenerated different proximodistal regions of the organ. Previous transcriptomic analyses of regenerating fins have focused on the early shifts in expression as the tissue initiates regenerative regrowth (Li et al., 2021; Nauroy et al., 2019); we found that there are substantial shifts in expression patterns even after regeneration is underway, as different stages of outgrowth proceed. Indeed, we found ten times as many distally, as compared to proximally, enriched transcripts; this may reflect the increased number of differentiated cells in the more mature regenerate as it returns to homeostatic growth (Nauroy et al., 2019).

The presence of TH throughout development distalizes gene expression patterns in intact fin tissues (Harper et al., 2023); however, during regeneration, thyroid status did not appear to influence expression along the regenerating proximodistal axis. The three stages analyzed in this study represent *both* expression differences associated with different amounts of time since injury *and* the regeneration of different proximodistal regions of the organ. It is possible that temporal shifts in the regenerating transcriptome may overwhelm any TH-dependent proximodistal pathways. Nevertheless, we identified many genes expressed in a proximodistal differential dependent on TH, and these are strong candidates for targets involved in distal patterning.

Notably, we did not identify any genes or pathways that were differentially expressed as the middle of the fin regenerated (where bifurcations actively form in WT fins). This suggests that there are not unique pathways underlying bifurcation, instead supporting a gradual distalization of regenerative gene expression along the proximodistal axis.

Tetrapod regeneration involves the readout of remembered proximodistal positional identity remembered by blastema cells (Stocum, 1984). In axolotls, distal blastema cells transplanted proximally exclusively rebuild distal structures (Pescitelli & Stocum, 1980), and these remembered positional identities are dependent on retinoic acid (Crawford & Stocum, 1988; Maden, 1982). While axolotls have revealed many proximodistal-defining factors, homologous mechanisms have not been found to regulate zebrafish regeneration (Rabinowitz et al., 2017).

Fin rays are known to retain memory of their original length (as shown in Shibata et al., 2018), however the existence of remembered identity along the proximodistal axis has not previously been demonstrated (Murciano et al., 2007; Shibata et al., 2018). Here, we demonstrated that proximally-transplanted distal portions of fin ray tissue produce regenerates that are influenced by retained memory of the original distal identity. Regenerates originating from dist-to-prox transplants retained a distal pattern of gene expression for a proximally-enriched transcript, initiated regeneration at a markedly slower pace, and regrew to a shorter length than expected for their location.

The growth rate and ultimate length of fin rays is known to be regulated by calcineurin bioelectric signaling pathways, which modulate local proliferation (Daane et al., 2018, 2021; Kujawski et al., 2014; Perathoner et al., 2014; Stewart et al., 2021; Tornini et al., 2016; Yi et al., 2021). Acutely inhibiting calcineurin causes lengthening of the regenerated organ (Kujawski et al., 2014) by accelerating growth rates (Daane et al., 2018). However, these changes in growth rate and ultimate length do not constitute changes in positional identity because they are not remembered in subsequent regeneration cycles (Daane et al., 2018). In contrast, reducing

proliferation in the blastema as regeneration is initiated can permanently change the memory of ultimate ray length, altering regenerate length through multiple rounds of regeneration (Wang et al., 2019).

Although dist-to-prox rays regenerated shorter than expected for their new environment, they regenerated much longer rays than the original size of the transplanted tissue, indicating that the proximal environment stimulated considerable growth in the regenerate. However, dist-to-prox regenerates grow to an ultimately shorter length than is appropriate for their regenerating environment, and this altered length phenotype is remembered through multiple rounds of regeneration. Previous proximodistal transplants of blastema cells or hemi-rays did not demonstrate any retained memory of these tissues, however these previous transplants were a combination of proximal and distal tissue (Murciano et al., 2007; Shibata et al., 2018). Intra-ray fibroblasts likely retain positional information (Perathoner et al., 2014); there may be a threshold of cells required to specify ray lengths, these effects diluted in previous transplant experiments by the mixed-identity tissues regenerating in a single ray. As our dist-to-prox transplantation relocates both bone and soft tissue, perhaps transplanted distal intra-ray fibroblasts remember proximodistal length information.

Speed of regeneration is specific to proximodistal location: proximal tissues regrows quickly while distal tissue regrows at a slower rate (Banu et al., 2022; Lee et al., 2005; Uemoto et al., 2020). Dist-to-prox rays regenerate at a slower pace during the first week of regrowth, suggesting a retained memory of distal identity. Thinner, smaller dist-to-prox rays provide fewer cells for the initial blastema proliferation, perhaps this smaller pool of cells is what determines the initial speed of regeneration and ultimately influences the total ray length during regeneration. This transient reduction is sufficient to permanently shorten the resulting ray even after homeostatic growth is achieved. As regrowth speed tapers off at a similar rate in all ray conditions, calcineurin signaling (Kujawski et al., 2014) and microRNA-133 expression (Yin et al., 2008) are most likely not autonomous to the tissue, as the transition from allometric (regenerative) to isometric (homeostatic) growth exclusively reflects the regenerative environment.

We recognized that the microsurgery alone had the potential to alter patterns of growth and length in regenerating tissue, and therefore we designed a “sham” baseline prox-to-prox surgery to isolate any effects of the extirpation and healing process. Importantly, the prox-to-prox rays regenerated somewhat more slowly and to a slightly shorter length compared to the corresponding ventral rays. This decreased growth rate may be caused by the loss of a few segments during microsurgery which may minimally distalize the ray. Wound healing occurring at the proximal end of the transplant could deprive blastemal tissue of resources at a local level, which might also explain these slight differences. Even compared to these controlled baselines, our dist-to-prox transplants showed significant reductions in growth rate and length, suggesting that these differences are genuinely due to the original identity of the tissue rather than the microsurgery alone.

Relative to intact dorsal rays, corresponding ventral rays were ‘proximalized,’ with bifurcations far from the body, longer and thicker segments. Furthermore, regeneration caused a moderate phenotypic proximalization, with bifurcations farther from the body (also shown in Azevedo et al., 2012) and somewhat thicker, longer segments. Thus, the prox-to-prox regenerates were the most appropriate comparisons to evaluate ray patterning. If proximodistal patterning is remembered autonomously, we would expect that dist-to-prox rays would regenerate with distal ray morphologies that are precocious relative to the environment (i.e. more proximal bifurcations and smaller, thinner segments). Previous work has suggested bifurcations are environmentally influenced (Dagenais et al., 2021; Murciano et al., 2002, 2007), and indeed prox-to-prox and dist-to-prox transplants bifurcated at a similar distance from the peduncle. Segment morphology also appears to be environmentally regulated, as segment lengths were indistinguishable between dist-to-prox and prox-to-prox rays. Although we

detected a small decrease in dist-to-prox segment width, we attributed it to the reduced population of regenerating cells in the thin distal graft.

CONCLUSION

In all, regenerating caudal fin tissue shows a graded change in expression patterns along the proximodistal axis, and hypothyroid fin tissue loses most of this differential expression. We found that proximodistal gene expression patterns could be remembered autonomously by the tissue, demonstrated by dist-to-prox transplants regenerating with diminished, distally appropriate levels of *scpp7* expression. Initial regenerative growth rates are informed by remembered tissue identity: dist-to-prox rays begin regeneration at a slow (distally appropriate) rate. Although the transplanted tissue later keeps pace with normal growth rates, the early setback maintains the ray originating from the transplant at a shorter length than its neighbors. Indeed, this shift in length is remembered through multiple rounds of regeneration.

MATERIALS AND METHODS

Fish rearing conditions. Zebrafish were reared at 28°C with a 14:10 light:dark cycle. Hypothyroid fish and their WT controls were *Tg(tg:nVenus-2a-nfnB)* (McMenamin et al., 2014). All other fish were WT (Tübingen line). WT fish were fed marine rotifers, *Artemia*, Gemma Micro (Skretting, Stavanger, NOR) and Adult Zebrafish Diet (Zeigler, Gardners PA, USA) 2-3 times per day. Hypothyroid fish and their WT controls were fed a diet of Spirulina flakes (Pentair, London, UK) and live *Artemia*.

Thyroid follicle ablations. To generate hypothyroid individuals, we performed transgenic thyroid ablations (as in McMenamin et al., 2014). Briefly, to ablate the thyroid follicles of *Tg(tg:nVenus-2a-nfnB)*, 4-5dpf larvae were incubated overnight in 10 mM metronidazole (Thermo Scientific Chemicals) dissolved in 1% dimethyl sulfoxide (DMSO, Sigma) in larval water, and controls with just 1% DMSO in larval water.

RNA Sequencing. Regenerating caudal fin tissue was collected from sibling adults (>18 standard length; SL) reared under wildtype or hypothyroid conditions during regeneration of three different regions. To minimize enrichment of genes involved in blastema formation (Li et al., 2021; Nauroy et al., 2019), we chose 4 dpa regenerates to represent proximal outgrowth. Tissue was collected at 4 dpa (proximal tissue), 7 dpa (middle tissue) or 15 dpa (distal tissue). Fish were anesthetized with tricaine (MS-222, Pentair; ~0.02% w/v in system water), the distal-most portion of the regenerating fin (~3 segments closest to the leading edge) was collected and immediately flash frozen in a dry ice / ethanol bath. Three or four biological replicates, each containing tissue from six individual fins, were collected at each time point and TH condition. Total RNA was extracted immediately with Zymo Quick-RNA Microprep kit R1050 (Zymo Research, Irvine CA, USA). Quality check, library preparation, and sequencing were performed by Genewiz (Cambridge, MA). Sample libraries were made with Illumina Truseq RNA Library Prep kit and sequenced on an Illumina HiSeq platform with 150bp paired-end sequence reads. Raw sequence reads were aligned to Zebrafish GRCz11 using STAR version 2.7.3 and gene counts were called with Ensembl GRCz11 gene annotation. Differential gene expression analyses were performed with Bioconductor package limma (Michaud et al., 2008). Genes were considered significantly expressed if they showed a $\log_2$ fold difference higher than 2 and a false discovery rate lower than 0.01.

Microsurgeries. Transplantation was most reliable using larger adults, so all individuals used for microsurgeries were 25-40mm SL. For ray extirpation, the entire dorsal ray four (DR4) was

removed. For dist-to-prox transplants, DR4 was extirpated from the fin, ~2 mm of the distal tip was clipped off, and this portion was grafted back into the now-empty DR4 site. For prox-to-prox transplants, DR4 was extirpated and then re-inserted in its native position. Directly after transplantation, fish were maintained in a lightly anesthetized state for 30-60 minutes using ~0.01% tricaine and 3PPM clove bud oil (Sigma-Aldrich). One day post-transplant, we assessed fins for graft success: dist-to-prox transplants grafted ~80% of the time while prox-to-prox transplants only grafted in ~60% of microsurgeries. After allowing 24 hours for recovery and for the graft to fuse with neighboring tissues, fish were again anesthetized with tricaine, and the entire fin (including the transplanted graft) was amputated along a single plane with a razor blade.

RNAscope whole mount *in situ* hybridization. Regenerating fins were collected at 4 dpa (proximal tissue or dist-to-prox tissue) or 15 dpa (distal tissue) and fixed for 30 minutes in 4% PFA at room temperature. Fins were stained as described in (I. Sehring et al., 2022) with the modification that all 0.2x SSCT washes were only performed twice. We used the RNAscope Multiplex Fluorescent Reagent Kit v2 (ACD Bio-techne, 323100) to screen seven candidate probes (ACD Bio-techne: *scpp7* 1265951-C1, *rhbg* 1315181-C2, *kcnma1a* 1315191-C3, *nfil3-6* 1265961-C2, *noxo1a* 1265971-C3, *defbl1* 1265981-C4, *olfml2ba* 1315201-C4) in proximal and distal regenerating tissue. Only the *scpp7* probe was able to reliably label transcripts in our whole mount tissues.

Imaging. Zebrafish were anesthetized with tricaine and imaged on an Olympus SZX16 stereoscope with an Olympus DP74 camera or an Olympus IX83 inverted microscope with a Hamamatsu ORCA Flash 4.0 camera. Identical microscope settings (including exposure and magnification) were used for all samples within each fluorescent *in situ* experiment. Images were transformed in FIJI with the Fire LUT for visualization. For fluorescent quantifications, we used FIJI to capture mean fluorescent intensity at the distal end of dorsal ray three, dorsal ray four transplant, and dorsal ray five (DR3, DR4, and DR5).

Analyses. All analyses were done in R 4.2.2. DR4 was used for all transplant procedures, with non-transplanted ventral ray four (VR4) serving as an internal comparison. Any damaged rays were excluded from analysis. Fin ray morphology was quantified with the StereoMorph R package (Olsen & Westneat, 2015) as described in (Harper et al., 2023). We used paired or unpaired Welch two-sample t tests or a paired repeated samples ANOVA followed by pairwise *t* tests to account for the two rays from a single fin or multiple time points assessed. Significance was marked as: $p < 0.05$, *; $p < 0.01$, **; $p < 0.001$, ***.

Pharmacological treatments. FK506 (Selleck Chemicals) was suspended in DMSO, then diluted to 200 nM FK506 and 0.02% DMSO. Controls were treated with 0.02% DMSO. ~70% water changes were performed every other day throughout the treatment before washout. Fish recovered for seven days, then were amputated a second time with no drug treatment.

AKNOLWEDGEMENTS
Thank you to all McMenamin Lab members past and present for fish care assistance. For data analysis support, we thank Melissa McTernan. For R assistance and dino nuggets, we thank Brian Autumn. For critical input and discussion, we thank Eric Folker, Matthew Harris, and Vicki Losick.

COMPETING INTERESTS
No competing interests declared.

FUNDING

NSF CAREER 1845513 and NIH R35GM146467 (S.K.M.).

DATA AVAILABILITY

All data is included in the article and supplementary materials.

GRAPHICAL ABSTRACT

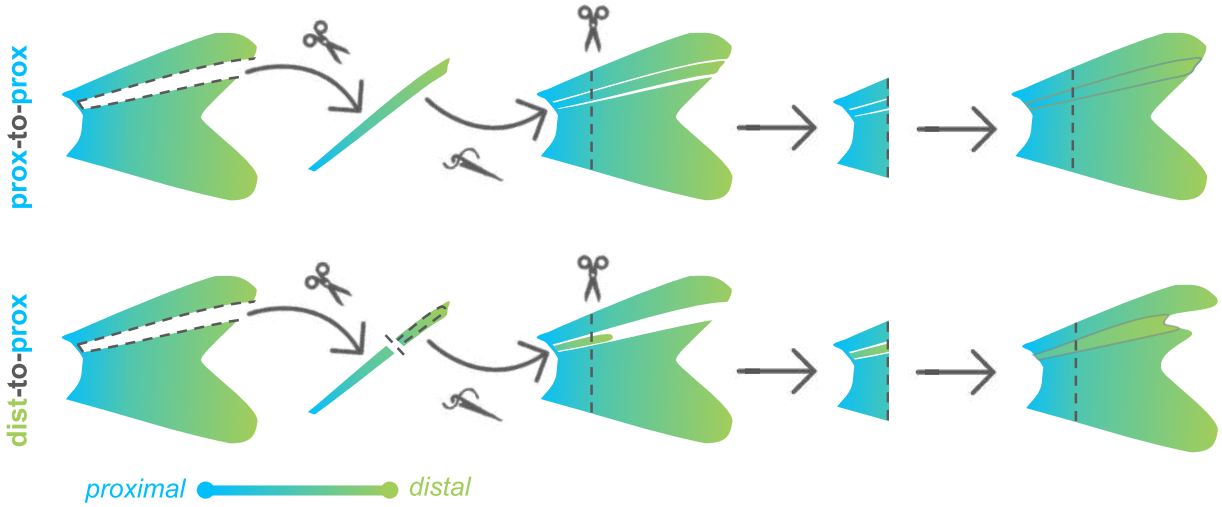

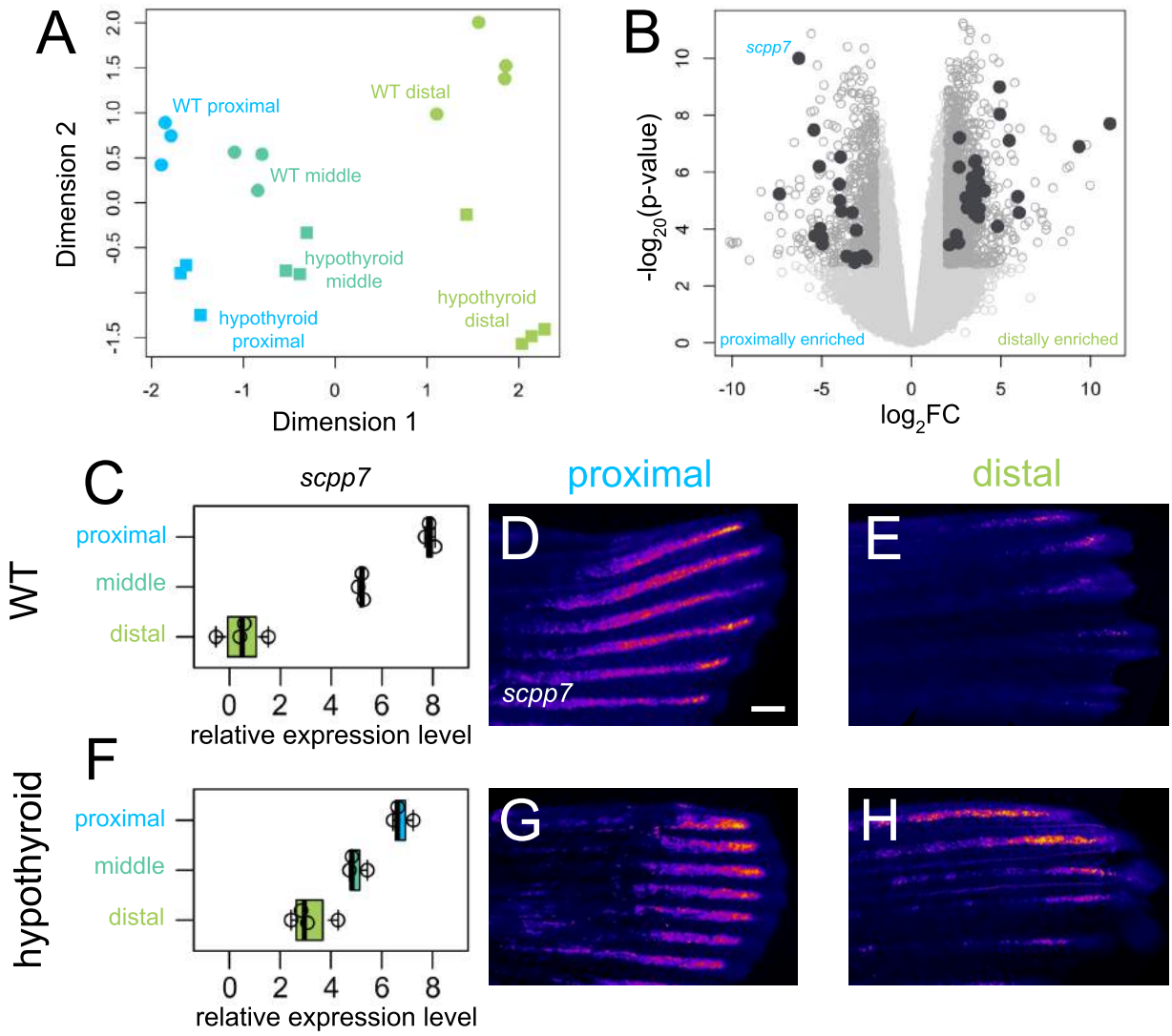

Figure 1. Thyroid hormone distalizes gene expression patterns during regeneration. (A) Multidimensional scaling plot comparing gene expression profiles in different regions (proximal, 4 dpa; middle, 7 dpa; distal, 15 dpa) of regenerating tissue from WT and hypothyroid fish; each data point represents one biological replicate. (B) Volcano plot showing differential gene expression between regenerating proximal and distal regions in WT. Filled grey circles indicate thyroid hormone-dependent genes. (D, F) *scpp7* relative expression in (C) WT and (F) hypothyroid tissue samples. Note increased proximal expression in hypothyroid distal tissues. Whole mount fluorescent *in situ* hybridization using custom *scpp7* RNAscope probe on (D-E) WT and (G-H) hypothyroid tissue regenerating (D, G) proximal or (E, H) distal fin tissues. Warm colors indicate highest regions of expression. Scale bar, 200 μm.

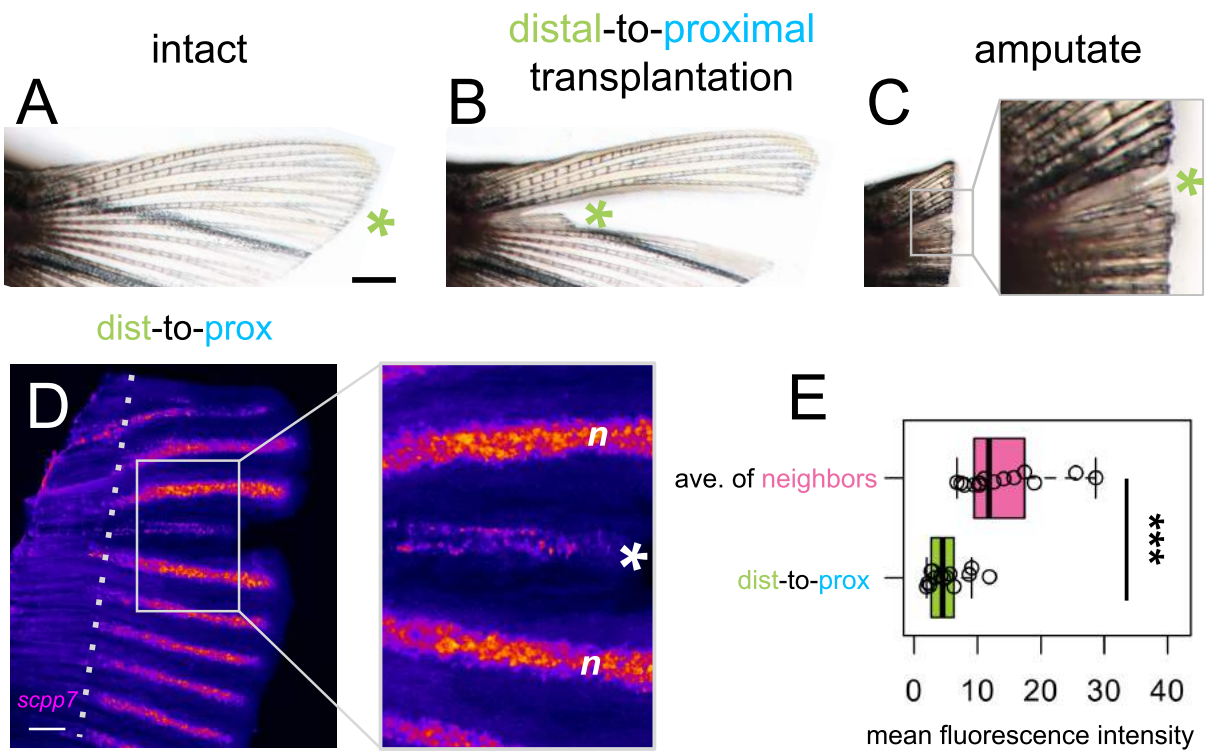

Figure 2. *scpp7* expression in regenerating tissues reflects original position rather than current environment. (A-C) Example of a fin lobe subjected to the distal-to-proximal transplantation procedure. (D) Whole mount fluorescent *in situ* hybridization with *scpp7* RNAscope probe on dist-to-prox regenerating fins at 4 dpa. Warm colors indicate highest regions of expression. (E) Boxplot showing mean fluorescence intensity of dist-to-prox transplant tissue (asterisk) and the average intensity of its peripheral-most and center-most neighbors (n). Significance determined by a Welch two-sample paired t test. Scale bars, (A) 1 mm; (D) 200 μm.

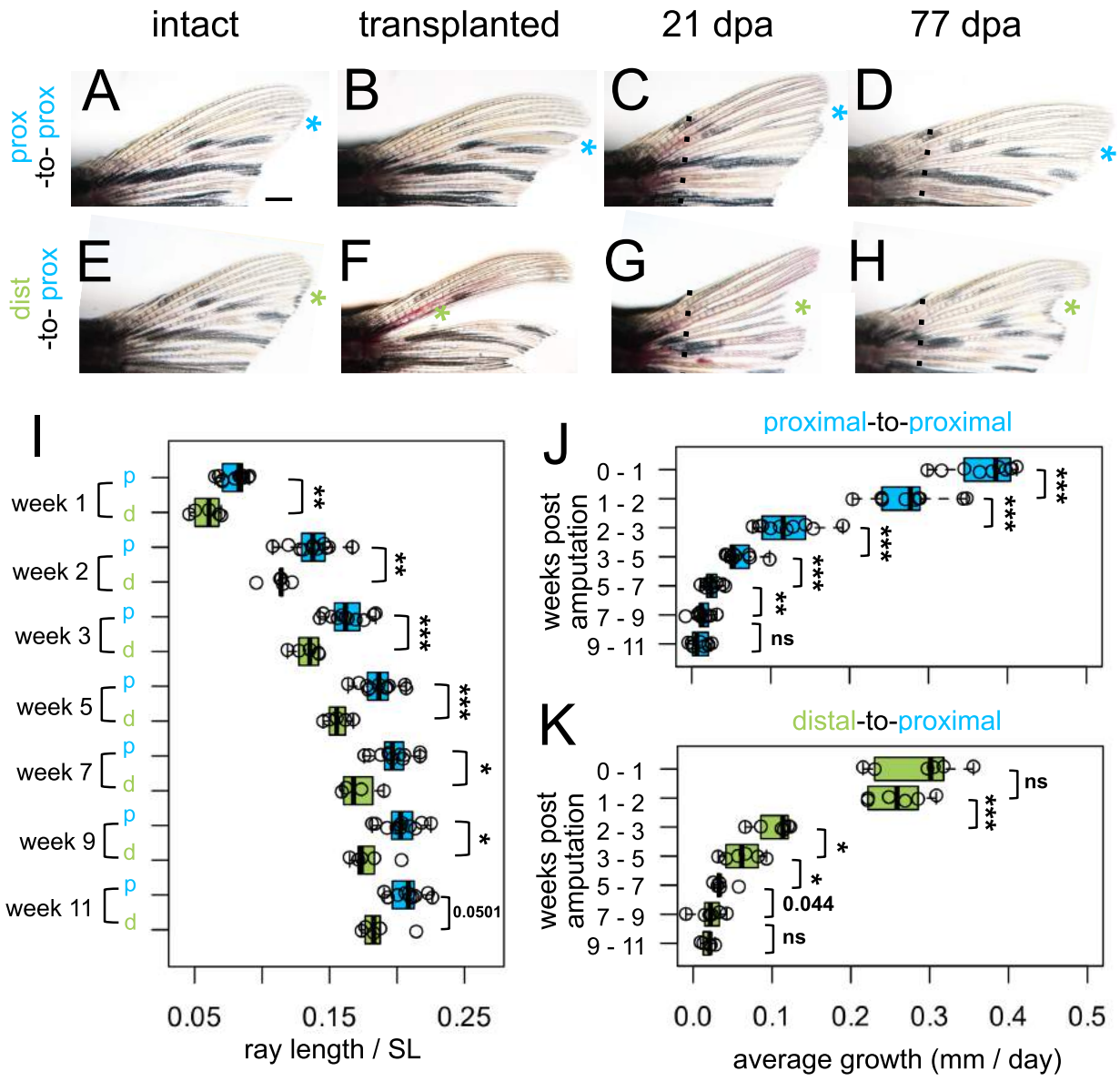

Figure 3. Regrowth rate reflects both intrinsic identity and the regenerative environment. Dorsal fin lobes of (A-D) proximal-to-proximal (blue asterisk) or (E-H) distal-to-proximal (green asterisk) transplantation: (A, E) intact pre-transplantation, (B-F) one day post-transplantation, (C-G) regenerating at 21 dpa, (D, H) regenerating at 77 dpa. Amputation plane, dashed line. (I) Prox-to-prox versus dist-to-prox ray length (measured from amputation plane) normalized by standard length (SL) for each week. Average amount of growth per day during different growth periods for (J) prox-to-prox or (K) dist-to-prox rays. Significance determined by (J-K) paired or (I) unpaired Welch two-sample t tests. Scale bar, 1 mm.

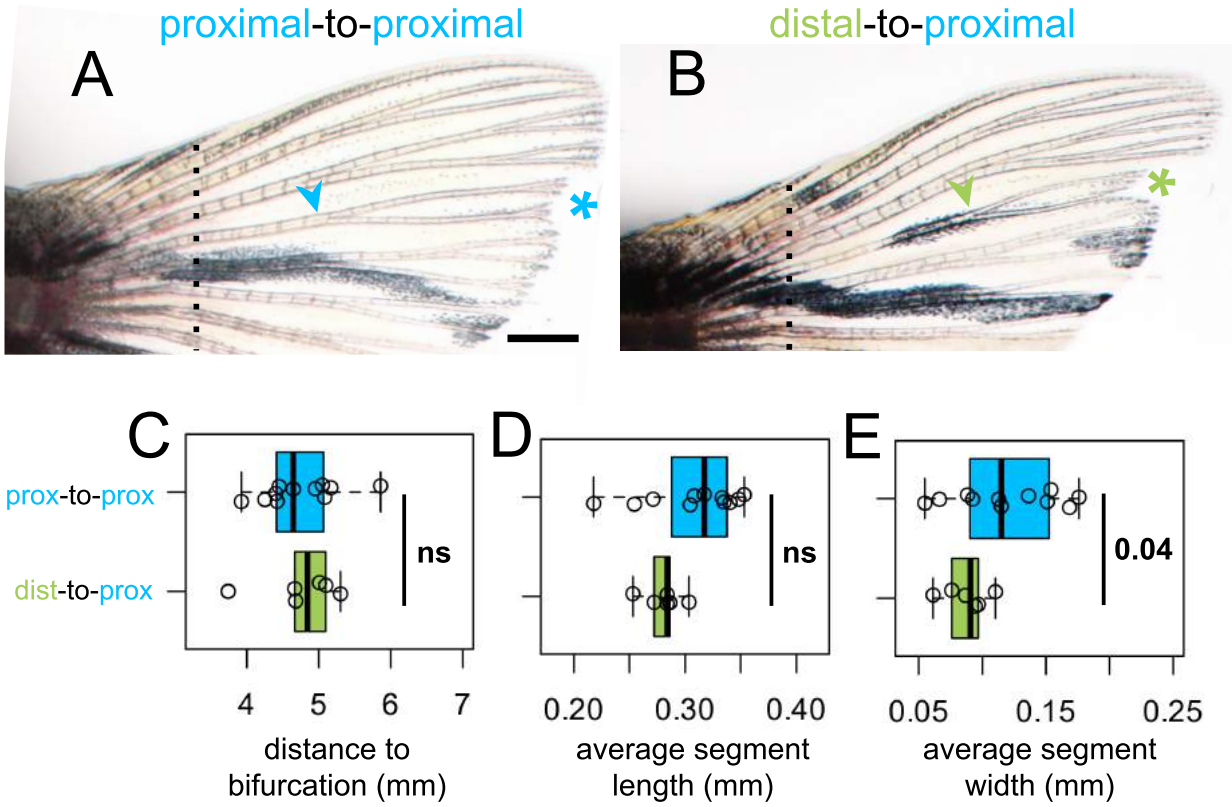

Figure 4. Fin ray patterning matches environment. Dorsal fin lobe at 35dpa after either (A) proximal-to-proximal (blue asterisk) or (B) distal-to-proximal (green asterisk) transplantation. Amputation plane shown with dashed line. Arrowheads indicate primary bifurcations. Boxplots showing the (C) proximodistal position of the bifurcation, (D) average segment length, and (E) average segment width in regenerate. Significance determined by a Welch two-sample t test. Scale bar, 1 mm.

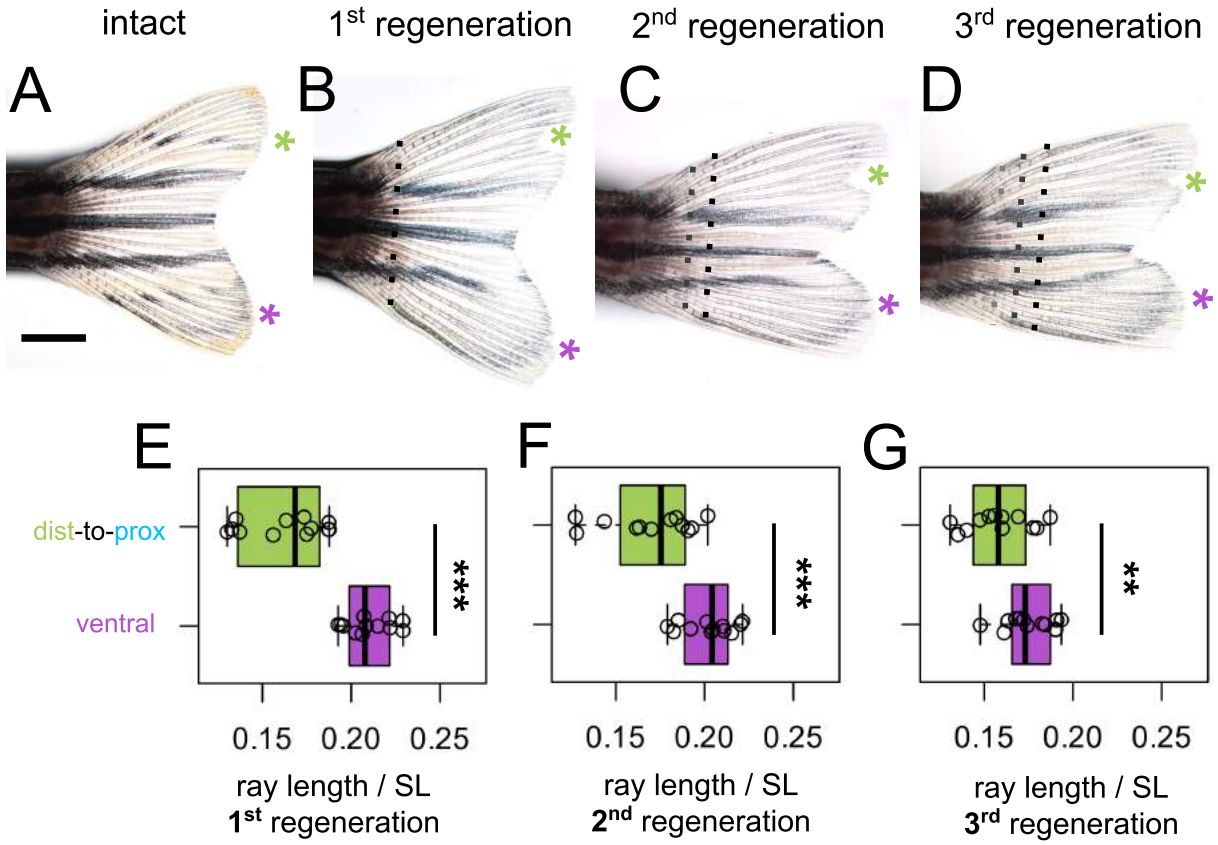

Figure 5. Shorter ray length is remembered through multiple regeneration cycles. (A) Intact fin. (B-D) Regenerating fin after distal-to-proximal transplantation: (B) 28 days post first amputation, (C) 28 days post second amputation, (C) 28 days post third amputation. Green asterisk, dist-to-prox; purple asterisk, ventral ray. Black dashed line, most recent amputation. Grey dashed lines, previous amputation planes. Boxplots showing the total length standardized by SL after (E) first, (F) second, and (G) third regeneration. Ray length was measured from the most recent amputation plane. Significance determined by paired Welch two-sample t test. Scale bar, 2 mm.

REFERENCES

Akimenko, M. A., Johnson, S. L., Westerfield, M., & Ekker, M. (1995). Differential induction of four msx homeobox genes during fin development and regeneration in zebrafish. *Development*, *121*(2), 347–357.

Azevedo, A. S., Sousa, S., Jacinto, A., & Saúde, L. (2012). An amputation resets positional information to a proximal identity in the regenerating zebrafish caudal fin. *BMC Developmental Biology*, *12*, 24. https://doi.org/10.1186/1471-213X-12-24

Banu, S., Gaur, N., Nair, S., Ravikrishnan, T., Khan, S., Mani, S., Bharathi, S., Mandal, K., Kuram, N. A., Vuppaladadium, S., Ravi, R., Murthy, C. L. N., Quoseena, M., Babu, N. S., & Idris, M. M. (2022). Understanding the complexity of epimorphic regeneration in zebrafish caudal fin tissue: A transcriptomic and proteomic approach. *Genomics*, *114*(2), 110300. https://doi.org/10.1016/J.YGENO.2022.110300

Bergen, D. J. M., Tong, Q., Shukla, A., Newham, E., Zethof, J., Lundberg, M., Ryan, R., Youlten, S. E., Frysz, M., Croucher, P. I., Flik, G., Richardson, R. J., Kemp, J. P., Hammond, C. L., & Metz, J. R. (2022). Regenerating zebrafish scales express a subset of evolutionary conserved genes involved in human skeletal disease. *BMC Biology 2021 20:1*, *20*(1), 1–25. https://doi.org/10.1186/S12915-021-01209-8

Crawford, K., & Stocum, D. L. (1988). Retinoic acid proximalizes level-specific properties responsible for intercalary regeneration in axolotl limbs. *Development*, *104*(4), 703–712. https://doi.org/10.1242/DEV.104.4.703

Daane, J. M., Blum, N., Lanni, J., Boldt, H., Iovine, M. K., Higdon, C. W., Johnson, S. L., Lovejoy, N. R., & Harris, M. P. (2021). Modulation of bioelectric cues in the evolution of flying fishes. *Current Biology*, *31*(22), 5052-5061.e8. https://doi.org/10.1016/J.CUB.2021.08.054

Daane, J. M., Lanni, J., Rothenberg, I., Seebohm, G., Higdon, C. W., Johnson, S. L., & Harris, M. P. (2018). Bioelectric-calcineurin signaling module regulates allometric growth and size of the zebrafish fin. *Scientific Reports 2018 8:1*, *8*(1), 1–9. https://doi.org/10.1038/s41598-018-28450-6

Dagenais, P., Blanchoud, S., Pury, D., Pfefferli, C., Aegerter-Wilmsen, T., Aegerter, C. M., & Jazwinska, A. (2021). Hydrodynamic stress and phenotypic plasticity of the zebrafish regenerating fin. *Journal of Experimental Biology*, *224*(15). https://doi.org/10.1242/JEB.242309/269186/AM/HYDRODYNAMIC-STRESS-AND-PHENOTYPIC-PLASTICITY-OF

Harper, M., Hu, Y., Donahue, J., Acosta, B., Braes, F. D., Nguyen, S., Zeng, J., Barbaro, J., Lee, H., Bui, H., & Mcmenamin, S. K. (2023). Thyroid hormone regulates proximodistal patterning in fin rays. *Proceedings of the National Academy of Sciences*, *120*(21), e2219770120. https://doi.org/10.1073/PNAS.2219770120

Harris, M. P., Daane, J. M., & Lanni, J. (2021). Through veiled mirrors: Fish fins giving insight into size regulation. *Wiley Interdisciplinary Reviews: Developmental Biology*, *10*(4). https://doi.org/10.1002/WDEV.381

Kawasaki, K. (2009). The SCPP gene repertoire in bony vertebrates and graded differences in mineralized tissues. *Development Genes and Evolution*, *219*(3), 147. https://doi.org/10.1007/S00427-009-0276-X

Knopf, F., Hammond, C., Chekuru, A., Kurth, T., Hans, S., Weber, C. W., Mahatma, G., Fisher, S., Brand, M., Schulte-Merker, S., & Weidinger, G. (2011). Bone regenerates via dedifferentiation of osteoblasts in the zebrafish fin. *Developmental Cell*, *20*(5), 713–724. https://doi.org/10.1016/j.devcel.2011.04.014

Kujawski, S., Lin, W., Kitte, F., Börmel, M., Fuchs, S., Arulmozhivarman, G., Vogt, S., Theil, D., Zhang, Y., & Antos, C. L. (2014). Calcineurin Regulates Coordinated Outgrowth of Zebrafish Regenerating Fins. *Developmental Cell*, *28*(5), 573–587. https://doi.org/10.1016/J.DEVCEL.2014.01.019

Lee, Y., Grill, S., Sanchez, A., Murphy-Ryan, M., & Poss, K. D. (2005). Fgf signaling instructs position-dependent growth rate during zebrafish fin regeneration. *Development*, *132*(23), 5173–5183. https://doi.org/10.1242/DEV.02101

Li, J., Sultan, Y., Sun, Y., Zhang, S., Liu, Y., & Li, X. (2021). Expression analysis of Hsp90α and cytokines in zebrafish caudal fin regeneration. *Developmental & Comparative Immunology*, *116*, 103922. https://doi.org/10.1016/J.DCI.2020.103922

Maden, M. (1982). Vitamin A and pattern formation in the regenerating limb. *Nature*, *295*.

McMenamin, S. K., Bain, E. J., McCann, A. E., Patterson, L. B., Eom, D. S., Waller, Z. P., Hamill, J. C., Kuhlman, J. A., Eisen, J. S., & Parichy, D. M. (2014). Thyroid hormone-dependent adult pigment cell lineage and pattern in zebrafish. *Science*, *345*(6202), 1358–1361. https://doi.org/10.1126/science.1256251

Michaud, J., Simpson, K. M., Escher, R., Buchet-Poyau, K., Beissbarth, T., Carmichael, C., Ritchie, M. E., Schütz, F., Cannon, P., Liu, M., Shen, X., Ito, Y., Raskind, W. H., Horwitz, M. S., Osato, M., Turner, D. R., Speed, T. P., Kavallaris, M., Smyth, G. K., & Scott, H. S. (2008). *Integrative analysis of RUNX1 downstream pathways and target genes*. https://doi.org/10.1186/1471-2164-9-363

Murciano, C., Fernández, T. D., Durán, I., Maseda, D., Ruiz-Sánchez, J., Becerra, J., Akimenko, M. A., & Marí-Beffa, M. (2002). Ray–Interray Interactions during Fin Regeneration of Danio rerio. *Developmental Biology*, *252*(2), 214–224. https://doi.org/10.1006/DBIO.2002.0848

Murciano, C., Pérez-Claros, J., Smith, A., Avaron, F., Fernández, T. D., Durán, I., Ruiz-Sánchez, J., García, F., Becerra, J., Akimenko, M. A., & Marí-Beffa, M. (2007). Position dependence of hemiray morphogenesis during tail fin regeneration in Danio rerio. *Developmental Biology*, *312*(1), 272–283. https://doi.org/10.1016/j.ydbio.2007.09.026

Nauroy, P., Guiraud, A., Chlasta, J., Malbouyres, M., Gillet, B., Hughes, S., Lambert, E., & Ruggiero, F. (2019). Gene profile of zebrafish fin regeneration offers clues to kinetics, organization and biomechanics of basement membrane. *Matrix Biology*, *75–76*, 82–101. https://doi.org/10.1016/J.MATBIO.2018.07.005

Olsen, A. M., & Westneat, M. W. (2015). StereoMorph: an R package for the collection of 3D landmarks and curves using a stereo camera set-up. *Methods in Ecology and Evolution*, *6*(3), 351–356. https://doi.org/10.1111/2041-210X.12326

Perathoner, S., Daane, J. M., Henrion, U., Seebohm, G., & Higdon, C. W. (2014). Bioelectric Signaling Regulates Size in Zebrafish Fins. *PLoS Genet*, *10*(1), 1004080. https://doi.org/10.1371/journal.pgen.1004080

Pescitelli, M. J., & Stocum, D. L. (1980). The origin of skeletal structures during intercalary regeneration of larval Ambystoma limbs. *Developmental Biology*, *79*(2), 255–275. https://doi.org/10.1016/0012-1606(80)90115-3

Rabinowitz, J. S., Robitaille, A. M., Wang, Y., Ray, C. A., Thummel, R., Gu, H., Djukovic, D., Raftery, D., Berndt, J. D., & Moon, R. T. (2017). Transcriptomic, proteomic, and metabolomic landscape of positional memory in the caudal fin of zebrafish. *Proceedings of the National Academy of Sciences of the United States of America*, *114*(5), E717–E726. https://doi.org/10.1073/pnas.1620755114

Sehring, I. M., & Weidinger, G. (2020). Recent advancements in understanding fin regeneration in zebrafish. *WIREs Developmental Biology*, *9*(1). https://doi.org/10.1002/wdev.367

Sehring, I., Mohammadi, H. F., Haffner-Luntzer, M., Ignatius, A., Huber-Lang, M., & Weidinger, G. (2022). Zebrafish fin regeneration involve generic and regeneration-specific osteoblast injury responses. *ELife*, *11*. https://doi.org/10.7554/ELIFE.77614

Shibata, E., Liu, Z., Kawasaki, T., Sakai, N., & Kawakami, A. (2018). Robust and local positional information within a fin ray directs fin length during zebrafish regeneration. *Development Growth and Differentiation*, *60*(6), 354–364. https://doi.org/10.1111/dgd.12558

Stewart, S., Le Bleu, H. K., Yette, G. A., Henner, A. L., Robbins, A. E., Braunstein, J. A., & Stankunas, K. (2021). longfin causes cis-ectopic expression of the kcnh2a ether-a-go-go K+ channel to autonomously prolong fin outgrowth. *Development (Cambridge)*, *148*(11). https://doi.org/10.1242/DEV.199384/260597/AM/LONGFIN-CAUSES-CIS-ECTOPIC-EXPRESSION-OF-THE

Stocum, D. L. (1984). The urodele limb regeneration blastema: Determination and organization of the morphogenetic field. *Differentiation*, *27*(1–3), 13–28. https://doi.org/10.1111/J.1432-0436.1984.TB01403.X

Tornini, V. A., Puliafito, A., Slota, L. A., Thompson, J. D., Nachtrab, G., Kaushik, A. L., Kapsimali, M., Primo, L., Di Talia, S., & Poss, K. D. (2016). Live Monitoring of Blastemal Cell Contributions during Appendage Regeneration. *Current Biology*, *26*(22), 2981–2991. https://doi.org/10.1016/j.cub.2016.08.072

Tu, S., & Johnson, S. L. (2011). Fate restriction in the growing and regenerating zebrafish fin. *Developmental Cell*, *20*(5), 725–732. https://doi.org/10.1016/j.devcel.2011.04.013

Uemoto, T., Abe, G., & Tamura, K. (2020). Regrowth of zebrafish caudal fin regeneration is determined by the amputated length. *Scientific Reports*, *10*(1), 649. https://doi.org/10.1038/s41598-020-57533-6

Wang, Y. T., Tseng, T. L., Kuo, Y. C., Yu, J. K., Su, Y. H., Poss, K. D., & Chen, C. H. (2019). Genetic Reprogramming of Positional Memory in a Regenerating Appendage. *Current Biology*, *29*(24), 4193-4207.e4. https://doi.org/10.1016/j.cub.2019.10.038

Wehner, D., Cizelsky, W., Vasudevaro, M. D., Özhan, G., Haase, C., Kagermeier-Schenk, B., Röder, A., Dorsky, R. I., Moro, E., Argenton, F., Kühl, M., & Weidinger, G. (2014). Wnt/β-catenin signaling defines organizing centers that orchestrate growth and differentiation of the regenerating zebrafish caudal fin. *Cell Reports*, *6*(3), 467–481. https://doi.org/10.1016/j.celrep.2013.12.036

Wolpert, L. (1969). Positional information and the spatial pattern of cellular differentiation. *Journal of Theoretical Biology*, *25*(1), 1–47. https://doi.org/10.1016/S0022-5193(69)80016-0

Yi, C., Spitters, T. W. G. M., Al-Far, E. A. D. A., Wang, S., Xiong, T., Cai, S., Yan, X., Guan, K., Wagner, M., El-Armouche, A., & Antos, C. L. (2021). A calcineurin-mediated scaling mechanism that controls a K+-leak channel to regulate morphogen and growth factor transcription. *ELife*, *10*. https://doi.org/10.7554/ELIFE.60691

Yin, V. P., Thomson, J. M., Thummel, R., Hyde, D. R., Hammond, S. M., & Poss, K. D. (2008). Fgf-dependent depletion of microRNA-133 promotes appendage regeneration in zebrafish. *Genes & Development*, *22*(6), 728. https://doi.org/10.1101/GAD.1641808

SUPPLEMENTARY FIGURES

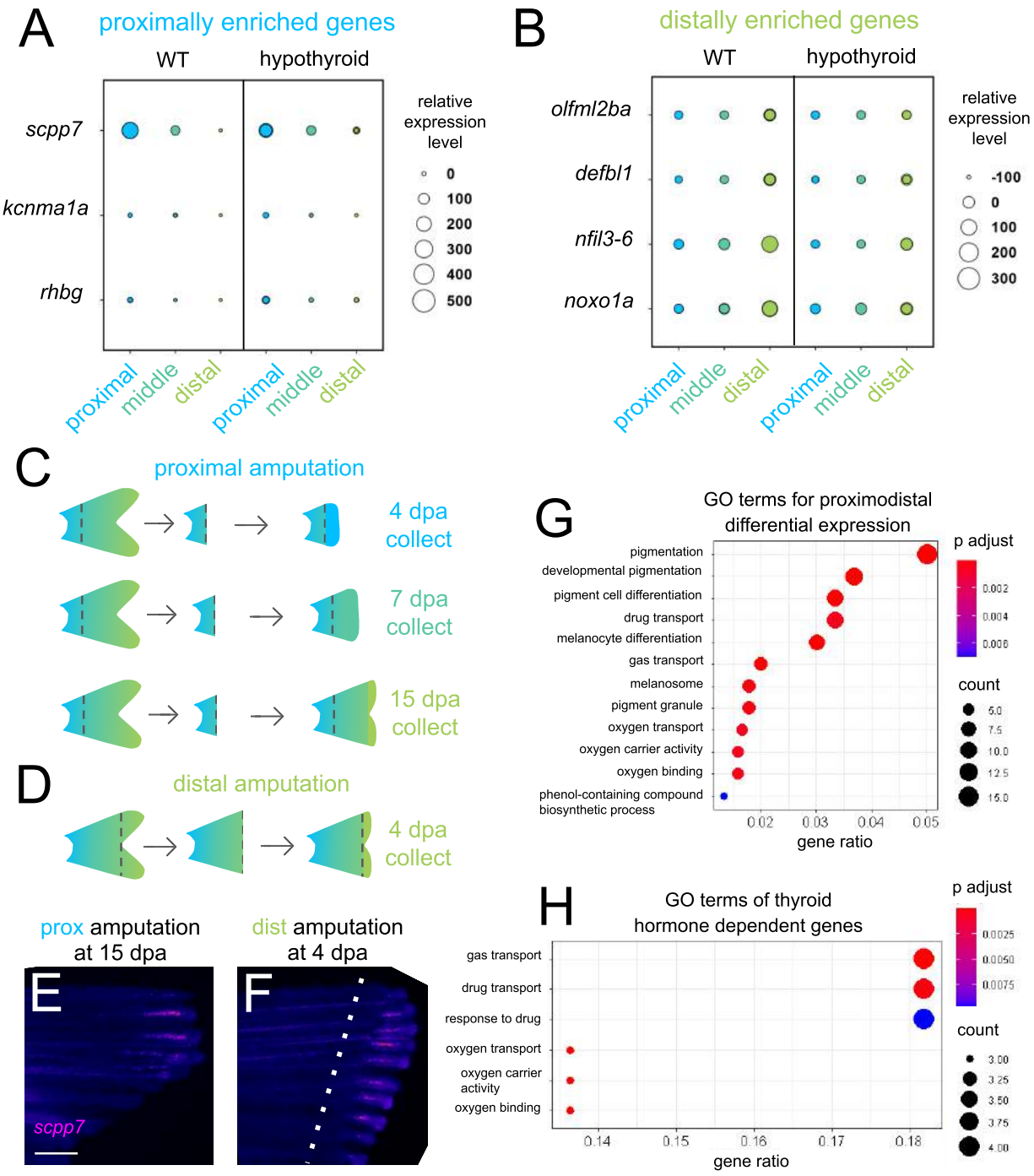

Supplementary Figure 1. Differentially expressed gene candidates for fluorescent *in situ* hybridization. Thyroid hormone-dependent gene candidates that are either (A) proximally enriched or (B) distally enriched in WT tissues. Custom RNAscope probes were made and tested for all genes, but only the *scpp7* probe showed specific staining. (C-D) Schematic

showing sample collection with (C) proximal or (D) distal amputation. (E) Proximally amputated at 15dpa or (F) distally amputated 4dpa tissue stained for *scpp7*. Amputation plane, dashed line. Warm colors indicate highest regions of expression. (G) GO enrichment of the 489 genes proximodistal differentially expressed in WT. (H) GO enrichment of the 45 genes that were thyroid hormone dependent and proximodistal differentially expressed in WT. Scale bar, 400 μm.

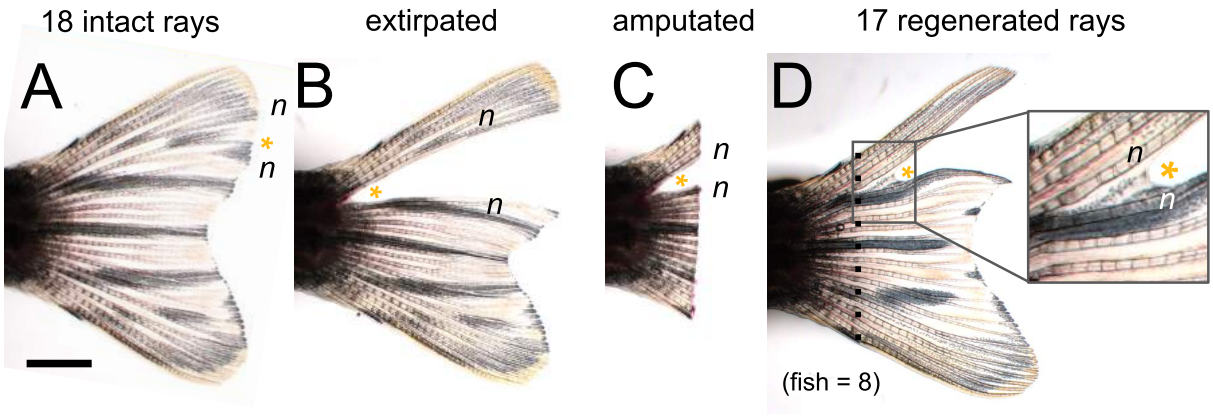

Supplementary Figure 2. Regeneration does not originate from an extirpated ray. (A) Intact fin with 18 rays, dorsal ray 4 (D4) marked with yellow asterisk. (B) Fin one day post D4 extirpation. (C) Freshly amputated fin, one day post D4 extirpation. (D) Fin regenerates with 17 rays (one-less ray than original, intact fin). n indicates neighboring dorsal rays 3 and 5. Amputation plane, dashed line. Scale bar, 2 mm.

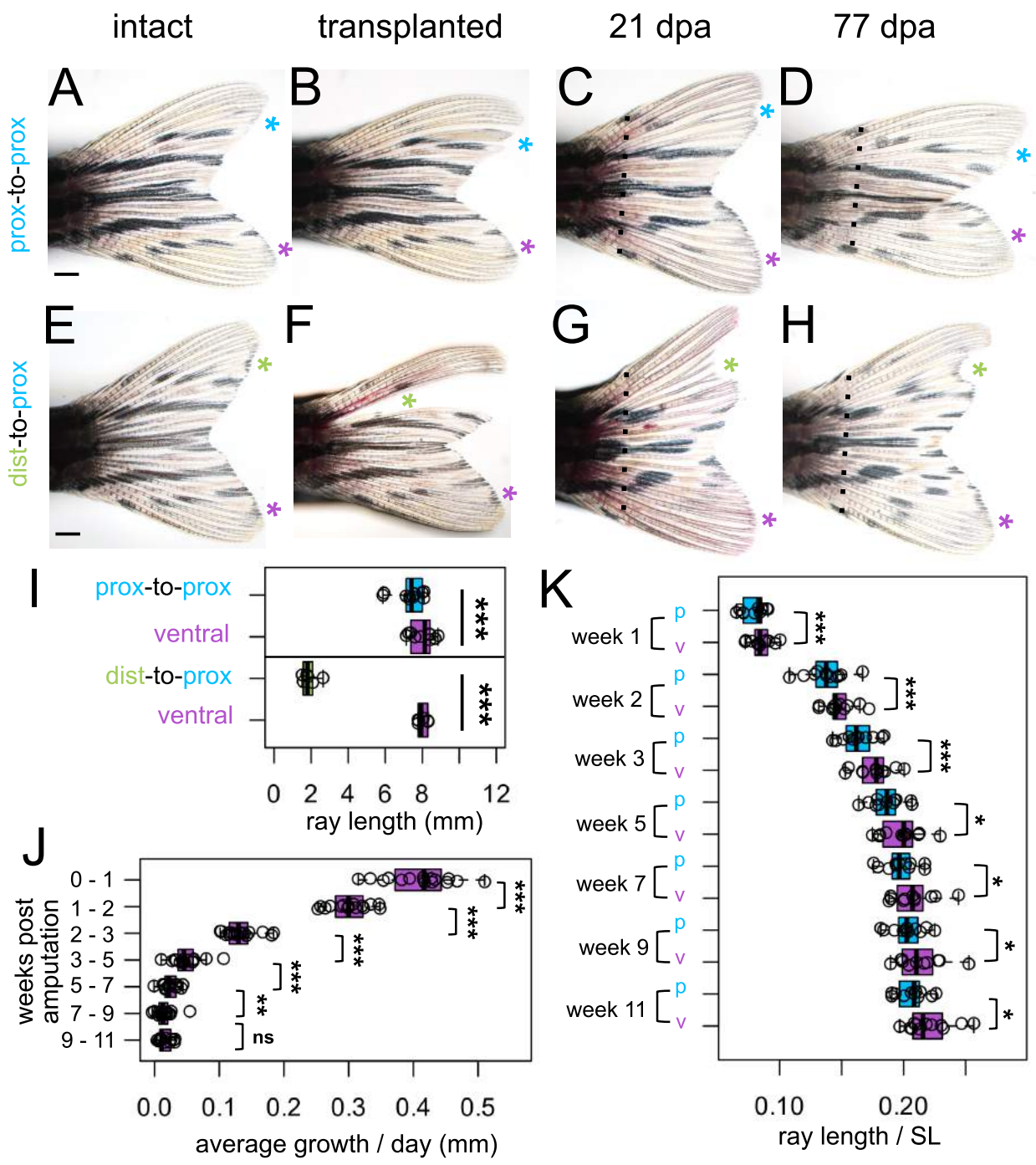

Supplementary Figure 3. Non-transplanted rays regenerated faster than transplanted rays. Fins of (A-D) proximal-to-proximal (blue asterisk) or (E-H) distal-to-proximal (green asterisk) transplantation: (A, E) intact pre-transplantation, (B-F) one day post-transplantation, (C-G) regenerating at 21 dpa, (D, H) regenerating at 77 dpa. Ventral rays indicated with purple asterisks. Amputation plane, dashed line. (I) Length of the rays after transplantation, as measured from the peduncle. (J) Average amount of growth per day during a one/two week periods for all the ventral ray comparisons. (K) Prox-to-prox rays versus ventral ray

comparisons, ray length (measured from amputation plane) divided by SL at each week. Significance determined by paired Welch two-sample t tests. Scale bar, 1 mm.

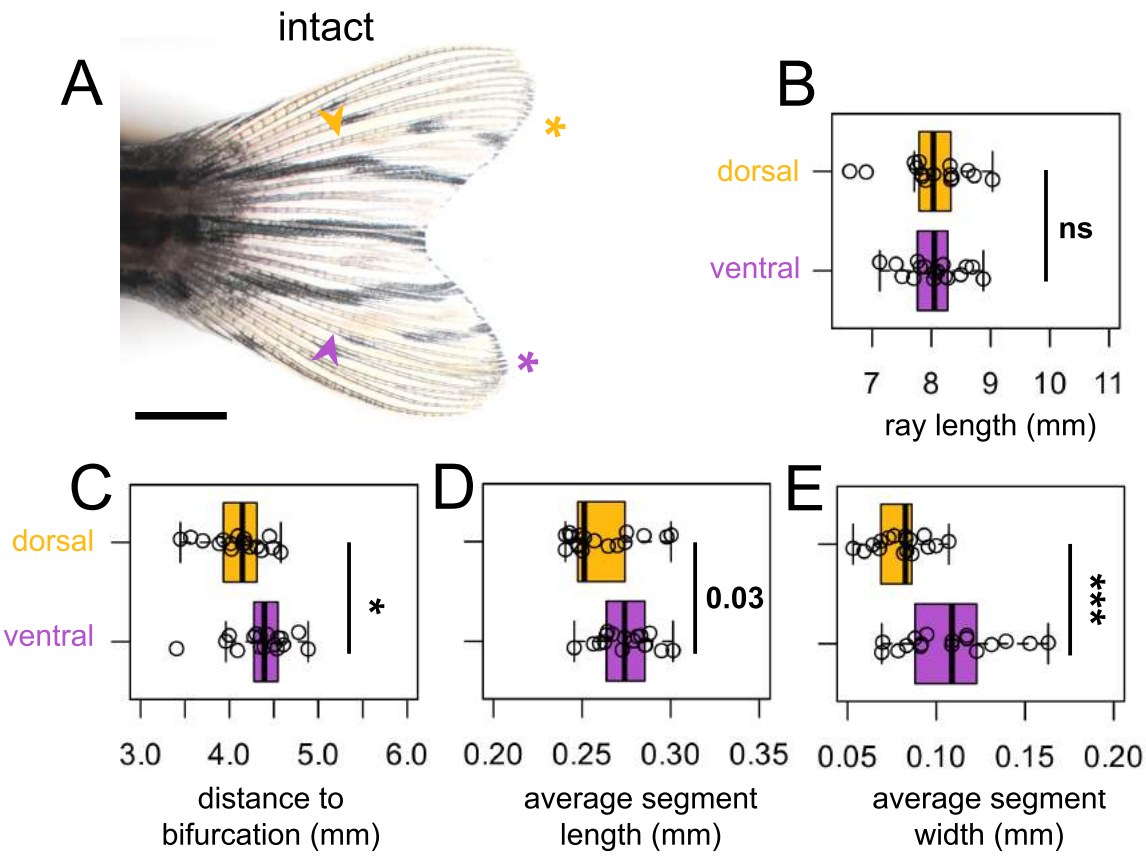

Supplementary Figure 4. Dorsal ray patterning is unique from ventral ray patterning. (A) Intact fin. A yellow or purple asterisk indicates dorsal ray 4 or ventral ray 4, respectively. Arrowheads, primary bifurcations. Boxplots showing the (B) total length of the ray, (C) proximodistal position of the bifurcation, (D) average segment length, and (E) average segment width measured from a set distance from the peduncle. Significance determined by a paired Welch two-sample t test. Scale bar, 2 mm.

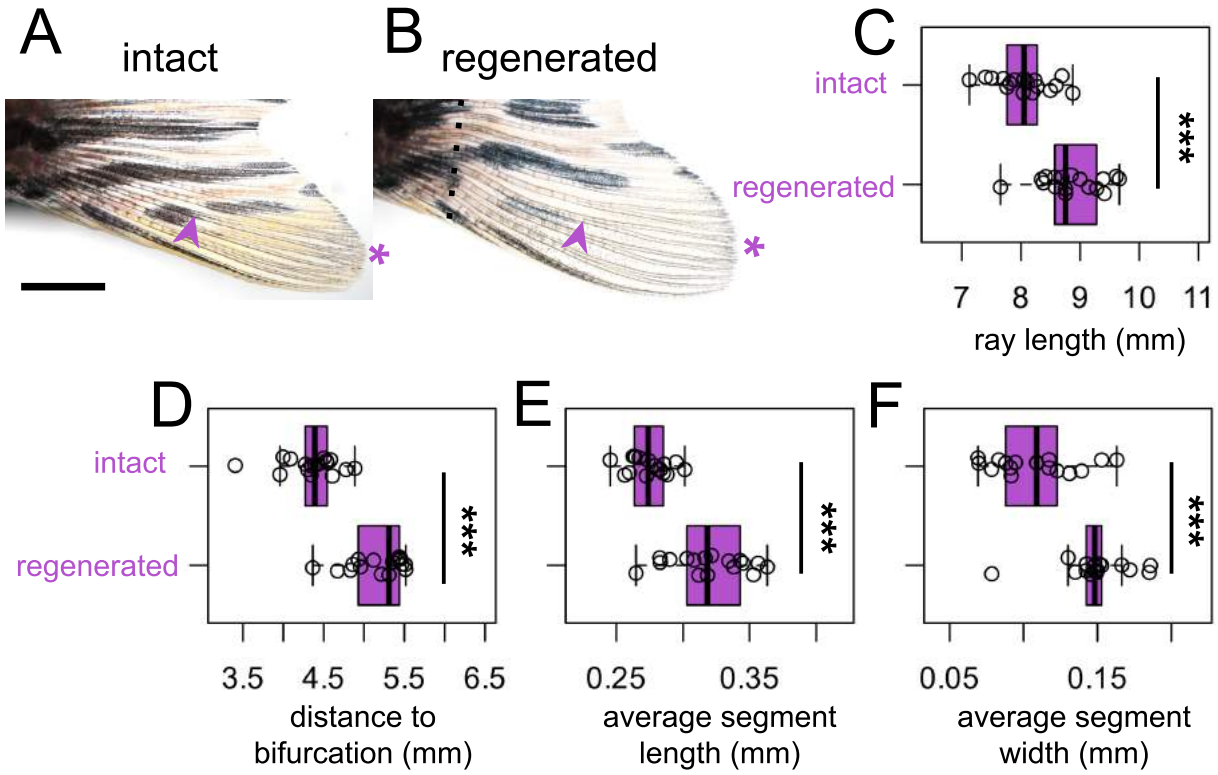

Supplementary Figure 5. Intact and regenerated ray patterning are different. (A-B) Ventral lobe of (A) intact or (B) regenerating fin at 35dpa. Purple asterisks indicate ventral ray 4. Arrowheads, primary bifurcations. Amputation plane, dashed line. Boxplots showing the (C) total length of the ray, (D) proximodistal position of the bifurcation, (E) average segment length, and (F) average segment width measured from a set distance from the peduncle. Significance determined by a paired Welch two-sample t test. Scale bar, 2 mm.

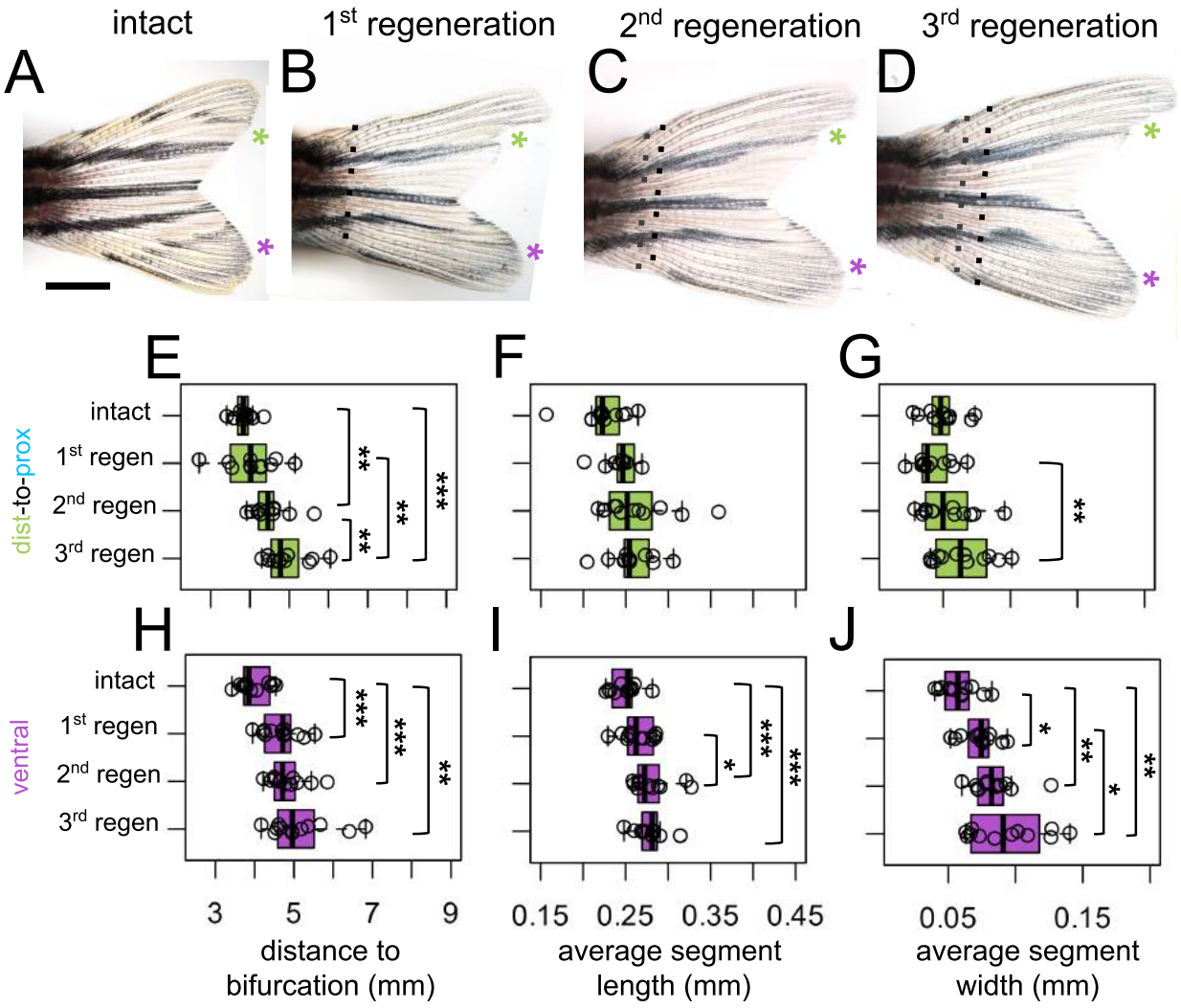

Supplementary Figure 6. Regenerative ray patterning differs from previous regenerated morphology. (A) Intact fin. (B-D) Regenerating fin after distal-to-proximal transplantation: (B) 28 days post first amputation, (C) 28 days post second amputation, (C) 28 days post third amputation. Green or purple asterisks indicate dist-to-prox or ventral ray, respectively. Black dashed line, most recent amputation. Grey dashed lines, previous amputation planes. (E, H) Boxplots showing the proximodistal position of the bifurcation. Note that bifurcations form at increasingly distal location after each amputation, as previously described . Boxplots showing (F, I) average segment length, and (G, J) average segment width. All measurements were taken from a set distance from the peduncle. Significance determined by paired repeated samples ANOVA followed by pairwise t tests. Scale bar, 2 mm.

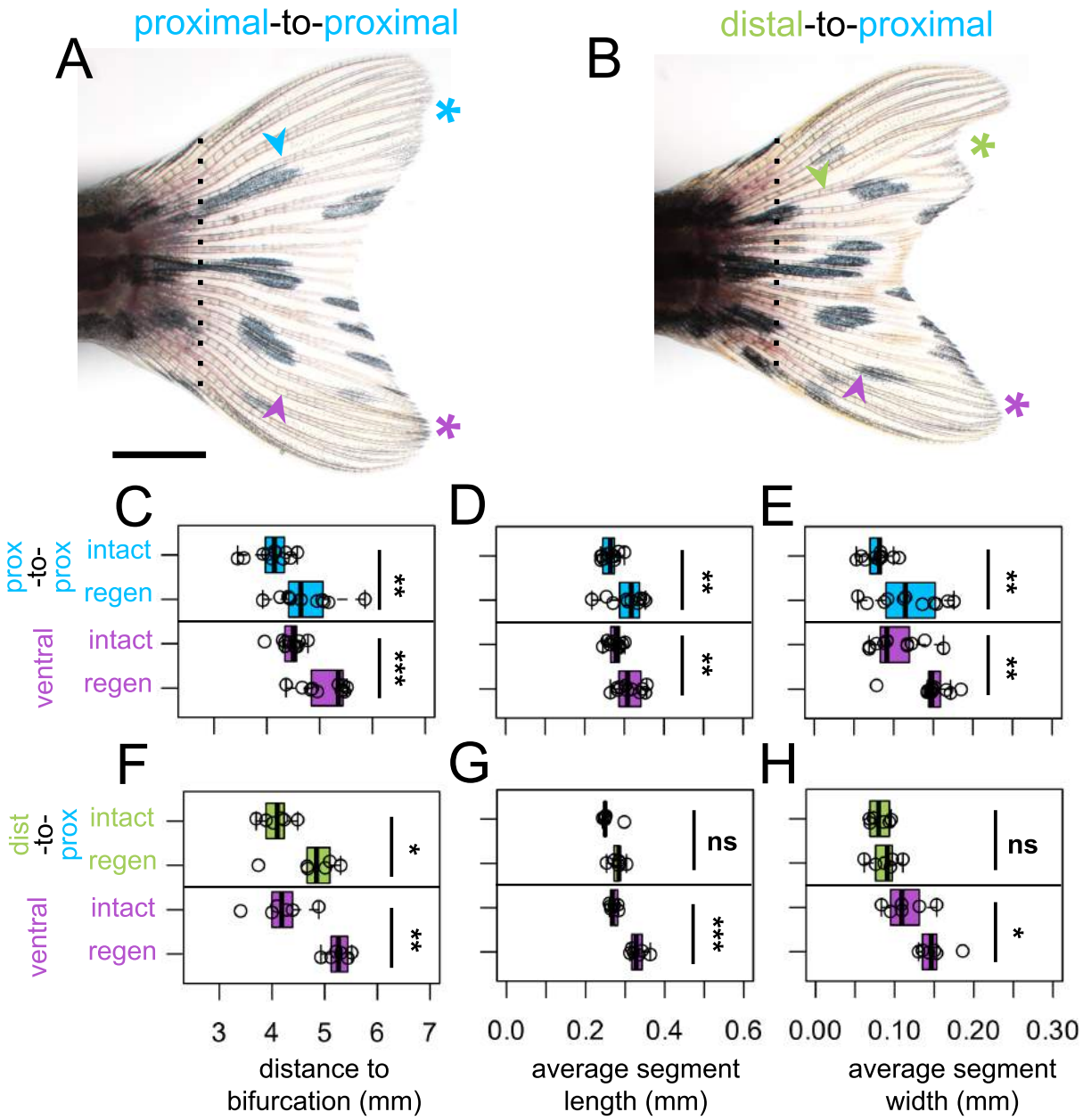

Supplementary Figure 7. Proximodistal patterning is dependent upon the current regenerative environment. Regenerating fins at 35dpa after either (A) proximal-to-proximal (blue asterisk) or (B) distal-to-proximal (green asterisk) transplantation. Purple asterisks indicate ventral ray comparison. Amputation plane shown with dashed line. Arrowheads indicate primary bifurcations. C-H) Boxplots showing the (C, F) proximodistal position of the bifurcation, (D, G) average segment length, and (E, H) average segment width of intact or regenerated rays, measured from a set distance from the peduncle. (C-E) Prox-to-prox or dist-to-prox ray measurements are shown alongside their ventral ray comparisons. Significance determined by a paired Welch two-sample t test. Scale bar, (A-B) 2 mm.

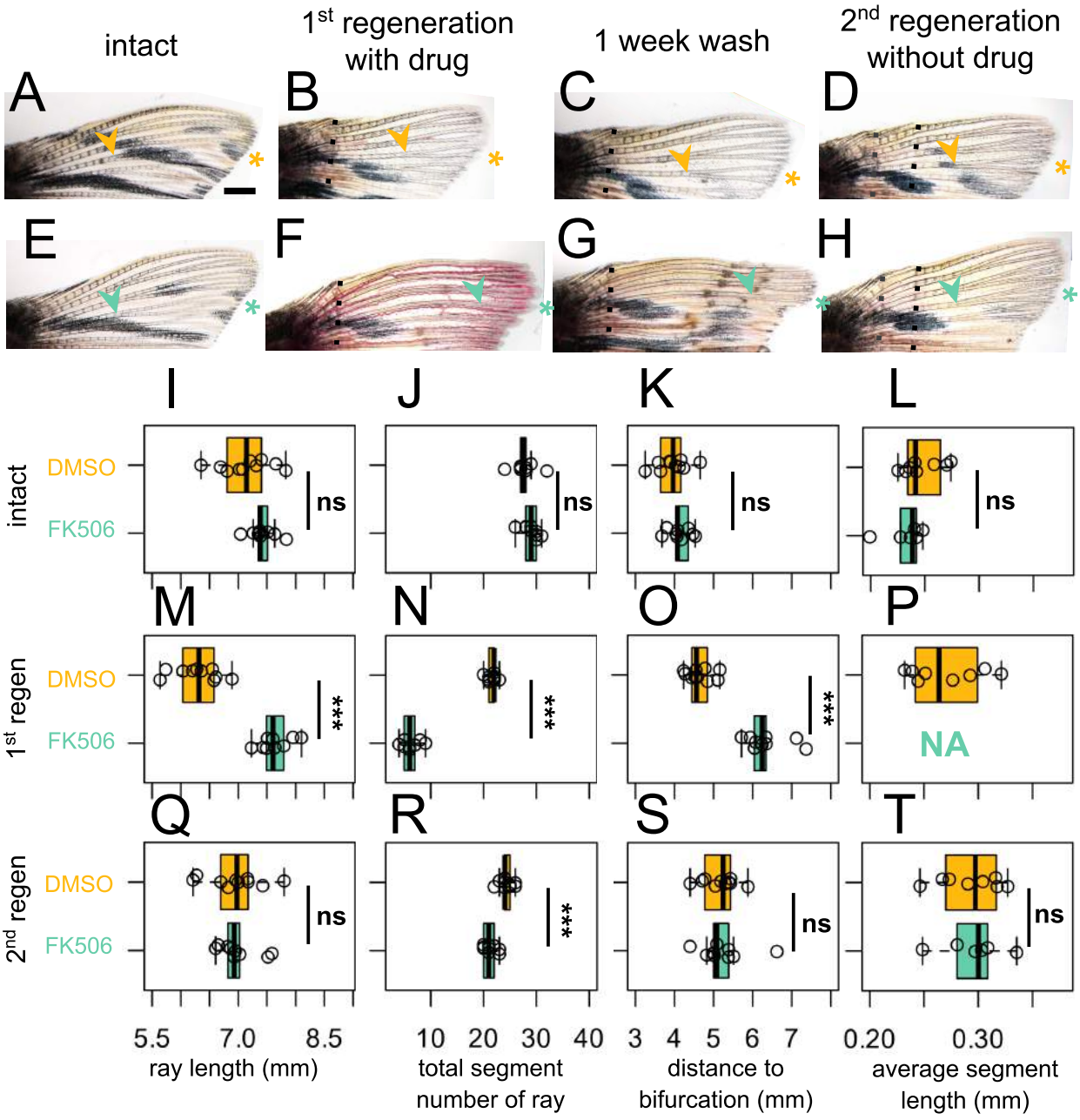

Supplementary Figure 8. Calcineurin inhibition-induced morphologies are not remembered in subsequent regeneration cycles. (A, E) Intact dorsal lobe before treatment. (B, F) Regenerated fin after (B) DMSO (yellow asterisk) or (F) 200 nM FK506 (turquoise asterisk) treatment, 21 days post amputation. (C, G) Fins after one week wash to clear remaining drug from water. (D, H) Regenerated fin 21 days post second amputation with no treatment. Black dashed line, most recent amputation. Grey dashed lines, previous amputation plane. Boxplots showing (I, M, Q) total ray length, (J, N, R) total number of segments of the ray, (K, O, S) bifurcation position, and (L, P, T) average segment length for (I-L) intact, (M-P) first regeneration with respective drug treatment, and (Q-T) second regeneration with no drug treatment. All measurements were taken from a set distance from the peduncle. Note in (P),

rays were built from only ~5 segments, making segments lengths so long that none were contained by the standard region of interest measured. Significance determined by unpaired Welch two-sample t test. Scale bar, 1 mm.